J|A|C|S
ARTICLES

Published on Web 01/21/2009

Spectroscopic Studies of the Light-Color Modulation Mechanism of Firefly (Beetle) Bioluminescence

Takashi Hirano,*,† Yosuke Hasumi,† Kazuhiro Ohtsuka,† Shojiro Maki,† Haruki Niwa,† Minoru Yamaji,‡ and Daisuke Hashizume§

Department of Applied Physics and Chemistry, The University of Electro-Communications, Chofu, Tokyo 182-8585, Japan, Department of Chemistry and Chemical Biology, Graduate School of Engineering, Gunma University, Kiryu, Gunma 376-8515, Japan, and Advanced Technology Support Division, RIKEN, Wako, Saitama 351-0198, Japan

Received November 11, 2008; E-mail: hirano@pc.uec.ac.jp

Abstract: To reveal the light-color modulation mechanism of firefly (beetle) bioluminescence, we investigated the spectroscopic properties of the phenolate anion **1**-O$^-$ generated from 5,5-dimethyloxyluciferin (**1**-OH) using various base/solvent combinations. Phenolate anion **1**-O$^-$ is a model compound for the keto form of wild-type oxyluciferin phenolate anion (OL$^-$), which is postulated to be the emitter of the bioluminescence. The fluorescence maxima of **1**-O$^-$ were found to depend on the base/solvent combination used, and they varied in the range 541−640 nm, which covers the almost whole range of the bioluminescence emission maximum. In a polar solvent, where ^{1}(**1**-O$^-$)* and the countercation (the conjugate acid of a base) make a solvent-separated ion pair or a free ion couple, the emission maxima of **1**-O$^-$ were found to be modulated by the solvent polarity. In a less polar solvent, where ^{1}(**1**-O$^-$)* and the countercation are formed as a contact ion pair, the strength of the covalent character of the O8′···H bond between ^{1}(**1**-O$^-$)* and the countercation is operative. The effect of the base/solvent combination on the emission properties of ^{1}(**1**-O$^-$)* was also verified using fluorescence lifetime measurements and density functional theory calculations on **1**-O$^-$ and its ion-pair models. On the basis of these results, we propose the following light-color modulation mechanism: (1) the light emitter is the excited singlet state of OL$^-$ [^{1}(OL$^-$)*], and (2) light emission from ^{1}(OL$^-$)* is modulated by the polarity of the active-site environment of a luciferase and the degree of covalent character of the O8′···H bond between ^{1}(OL$^-$)* and a protonated basic moiety in the active site. Mechanisms for variation of the bioluminescence colors and their applications are discussed.

Introduction

Fireflies and their analogous beetles (click beetles and railroad worms)[1] generate light by luciferin−luciferase reactions (Scheme 1).[2−4] Under enzymatic regulation by a luciferase, firefly luciferin (LH_2) reacts with ATP and molecular oxygen (O_2) in the presence of Mg^{2+} to give oxyluciferin (OLH) and a photon, accompanied by CO_2, AMP, and pyrophosphate (PPi). The important characteristics of the firefly (beetle) luminescence system[1] are the requirement of ATP,[5] large quantum yields of light production,[6] and photon generation over a wide range of colors from green to red (emission maxima in the range 530−640 nm).[7−9] On the basis of these well-established functions, applications of firefly (beetle) bioluminescence in

Scheme 1

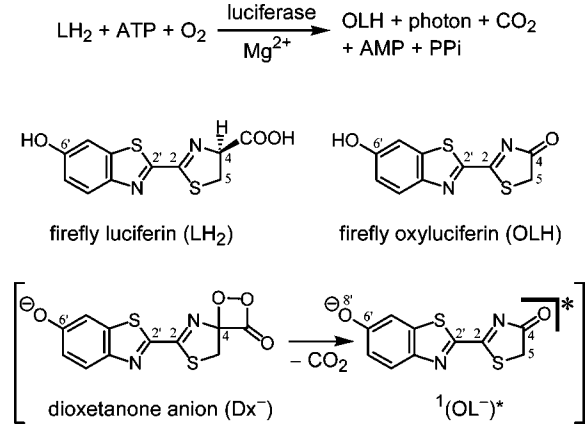

† The University of Electro-Communications.
‡ Gunma University.
§ RIKEN.

(1) In this paper, we use the term "firefly (beetle) bioluminescence" for the bioluminescence of fireflies, click beetles, and railroad worms. The word "beetle bioluminescence" has also been used.
(2) McElroy, W. D.; DeLuca, M. In *Bioluminescence in Action*; Herring, P. J., Ed.; Academic Press: London, 1978; pp 109−127.
(3) Shimomura, O. In *Bioluminescence: Chemical Principles and Methods*; World Scientific Publishing: Singapore, 2006; pp 1−29.
(4) Fraga, H. *Photochem. Photobiol. Sci.* **2008**, *7*, 146–158.
(5) McElroy, W. D. *Proc. Natl. Acad. Sci. U.S.A.* **1947**, *33*, 342–345.
(6) (a) Seliger, H. H.; McElroy, W. D. *Biochem. Biophys. Res. Commun.* **1959**, *1*, 21–24. (b) Seliger, H. H.; McElroy, W. D. *Arch. Biochem. Biophys.* **1960**, *88*, 136–141.
(7) Seliger, H. H.; McElroy, W. D. *Proc. Natl. Acad. Sci. U.S.A.* **1964**, *52*, 75–81.
(8) (a) Wood, K. V.; Lam, Y. A.; Seliger, H. H.; McElroy, W. D. *Science* **1989**, *244*, 700–703. (b) Wood, K. V.; Lam, Y. A.; McElroy, W. D. *J. Biolumin. Chemilumin.* **1989**, *4*, 289–301.
(9) Viviani, V. R. *Cell. Mol. Life Sci.* **2002**, *59*, 1833–1850.

10.1021/ja808836b CCC: $40.75

biological science are expanding.[10−13] To develop the usefulness of the bioluminescence system, we must understand its fundamental chemistry. Recent research has clarified several important subjects, including the quantum yield[14] and the complex structures of luciferase and substrates.[15,16] In contrast, the light-color modulation mechanism is still unclear.

Since LH_2 is the common bioluminescence center for fireflies and their analogous beetles,[7] the color variation must correspond to changes in the structure and/or properties of the excited molecule of OLH modulated by the molecular environment of the active site of the luciferase (Scheme 1). In the last four decades, several mechanisms have been proposed to explain the multicolor bioluminescence of fireflies (beetles).[16−24] The proposed candidates for the light-emitter structure are the keto form of oxyluciferin phenolate anion (OL^-), its enol isomer, and the dianion having phenolate and enolate moieties.[17−19] In addition, it has been proposed that the excited singlet state of OL^- [$^1(OL^-)^*$] has a twisted structure with intramolecular charge transfer (ICT) character, where the benzothiazole and thiazolone rings are perpendicular as a result of rotation around the C2−C2′ bond.[20] In 2002, Branchini et al.[21] reported one of solutions for the problem of the light-emitter structure. They found that the bioluminescence of the adenylate of 5,5-dimethylluciferin can generate various colors of light. The product of the bioluminescence reaction of 5,5-dimethylluciferin adenylate must be 5,5-dimethyloxyluciferin (**1**-OH), which is unable to provide its enol and enolate species. On the basis of this finding, $^1(OL^-)^*$ becomes the most plausible candidate for the light-emitter structure in the excited singlet state during firefly (beetle) bioluminescence. This conclusion is also consistent with the reaction mechanism in which $^1(OL^-)^*$ is the primary product of the chemiexcitation process from the anionic

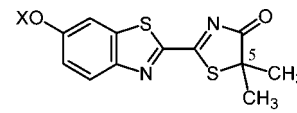

1-OH: X = H
1-OCH_3: X = CH_3

dioxetanone intermediate (Dx^-), as shown in Scheme 1.[25−28] Therefore, it is reasonable to postulate that the color variation originates from modulation of the emission properties of $^1(OL^-)^*$ in the active site of a luciferase. Changes in the $^1(OL^-)^*$ emission properties have been explained by the use of the resonance structures of OL^-, which have π-electron conjugation between the benzothiazole and thiazolone rings.[22] Furthermore, we must consider environmental factors surrounding $^1(OL^-)^*$. The pioneering studies by Seliger and co-workers[23] and DeLuca[24] emphasize that the polarity of the active-site environment is operative in modulating the bioluminescence color. It has also been proposed that the position of a basic moiety (such as an arginine residue) in the vicinity of $^1(OL^-)^*$ is a factor affecting the resonance properties of OL^-.[22] In addition, a recent crystallographic study on a luciferase and its mutants proposed another mechanism: the bioluminescence color is modulated by the rigidity of the active site, which regulates the vibrational energy loss of $^1(OL^-)^*$.[16]

To reveal the light-color modulation mechanism with reference to these previous studies, much attention has been paid to the fluorescence properties of OL^-.[18,19,29,30] Although the elucidation of the spectroscopic properties of OL^- may contribute to understanding the light-color modulation mechanism, its spectroscopic properties have not been investigated directly because of its low thermal stability. In particular, OLH has acidic α-hydrogens at C5 that provide corresponding enol and enolate species. Thus, it is preferable to employ **1**-OH for studying the fluorescence of phenolate anion free from the participation of enol and enolate species. On the basis of this idea, the fluorescence of **1**-O^-, the phenolate anion of **1**-OH, has been investigated by several research groups.[19,31,32] However, a systematic understanding of the properties of ^{1}(**1**-O^-)* is still incomplete. Here we report a study of the spectroscopic properties of **1**-O^- in comparison with those of **1**-OH and its methyl ether derivative **1**-OCH_3.[33,34] The goal of the present study is to understand the emission properties of ^{1}(**1**-O^-)* and how they are affected by the solvent polarity and a bonding interaction with a countercation. The results obtained provide evidence for the light-color modulation mechanism. Application

(10) DeLuca, M.; McElroy, W. D. *Methods Enzymol.* **1978**, *57*, 3–15.
(11) (a) de Wet, J. R.; Wood, K. V.; Helinski, D. R.; DeLuca, M. *Proc. Natl. Acad. Sci. U.S.A.* **1985**, *82*, 7870–7873. (b) de Wet, J. R.; Wood, K. V.; Helinski, D. R.; DeLuca, M. *Methods Enzymol.* **1986**, *133*, 3–14.
(12) Greer, L. F.; Szalay, A. A. *Luminescence* **2002**, *17*, 43–74.
(13) Contag, C. H.; Bachmann, M. H. *Annu. Rev. Biomed. Eng.* **2002**, *4*, 235–260.
(14) Ando, Y.; Niwa, K.; Yamada, N.; Enomoto, T.; Irie, T.; Kubota, H.; Ohmiya, Y.; Akiyama, H. *Nat. Photonics* **2008**, *2*, 44–47.
(15) Conti, E.; Franks, N. P.; Brick, P. *Structure* **1996**, *4*, 287–298.
(16) Nakatsu, T.; Ichiyama, S.; Hiratake, J.; Saldanha, A.; Kobashi, N.; Sakata, K.; Kato, H. *Nature* **2006**, *440*, 372–376.
(17) (a) White, E. H.; Rapaport, E.; Hopkins, T. A.; Seliger, H. H. *J. Am. Chem. Soc.* **1969**, *91*, 2178–2180. (b) White, E. H.; Steinmetz, M. G.; Miano, J. D.; Wildes, P. D.; Morland, R. *J. Am. Chem. Soc.* **1980**, *102*, 3199–3208.
(18) White, E. H.; Rapaport, E.; Seliger, H. H.; Hopkins, T. A. *Bioorg. Chem.* **1971**, *1*, 92–122.
(19) White, E. H.; Roswell, D. F. *Photochem. Photobiol.* **1991**, *53*, 131–136.
(20) (a) McCapra, F.; Gilfoyle, D. J.; Young, D. W.; Church, N. J.; Spencer, P. In *Bioluminescence and Chemiluminescence. Fundamentals and Applied Aspects*; Campbell, A. K., Kricka, L. J., Stanley, P. E., Eds.; Wiley: Chichester, U.K., 1994; pp 387−391. (b) McCapra, F. In *Bioluminescence and Chemiluminescence: Molecular Reporting with Photons*; Hastings, J. W., Kricka, L. J., Stanley, P. E., Eds.; Wiley: Chichester, U.K., 1997; pp 7−15.
(21) Branchini, B. R.; Murtiashaw, M. H.; Magrar, R. A.; Portier, N. C.; Ruggiero, M. C.; Stroh, J. G. *J. Am. Chem. Soc.* **2002**, *124*, 2112–2113.
(22) Branchini, B. R.; Southworth, T. L.; Murtiashaw, M. H.; Magrar, R. A.; Gonzalez, S. A.; Ruggiero, M. C.; Stroh, J. G. *Biochemistry* **2004**, *43*, 7255–7262.
(23) Morton, R. A.; Hopkins, T. A.; Seliger, H. H. *Biochemistry* **1969**, *8*, 1598–1607.
(24) DeLuca, M. *Biochemistry* **1969**, *8*, 160–166.
(25) Hopkins, T. A.; Seliger, H. H.; White, E. H.; Cass, M. W. *J. Am. Chem. Soc.* **1967**, *89*, 7148–7150.
(26) McCapra, F.; Chang, Y. C.; François, V. P. *Chem. Commun.* **1968**, 22–23.
(27) Shimomura, O.; Goto, T.; Johnson, F. H. *Proc. Natl. Acad. Sci. U.S.A.* **1977**, *74*, 2799–2802.
(28) Wannlund, J.; DeLuca, M.; Stempel, K.; Boyer, P. D. *Biochem. Biophys. Res. Commun.* **1978**, *81*, 987–992.
(29) (a) Suzuki, N.; Sato, M.; Nishikawa, K.; Goto, T. *Tetrahedron Lett.* **1969**, *10*, 4683–4684. (b) Suzuki, N.; Sato, M.; Okada, K.; Goto, T. *Tetrahedron* **1972**, *28*, 4065–4074.
(30) (a) Gandelman, O. A.; Brovko, L. Y.; Ugarova, N. N.; Shchegolev, A. A. *Biochemistry (Moscow)* **1990**, *55*, 785–789. (b) Gandelman, O. A.; Brovko, L. Y.; Ugarova, N. N.; Chikishev, A. Y.; Shkurimov, A. P. *J. Photochem. Photobiol., B* **1993**, *19*, 187–191.
(31) Suzuki, N.; Ueyama, T.; Izawa, Y.; Toya, Y.; Goto, T. *Heterocycles* **1983**, *20*, 1027–1030.
(32) (a) Leontieva, O. V.; Vlasova, T. N.; Ugarova, N. N. *Biochemistry (Moscow)* **2006**, *71*, 51–55. (b) Vlasova, T. N.; Leontieva, O. V.; Ugarova, N. N. *Biochemistry (Moscow)* **2006**, *71*, 555–559.

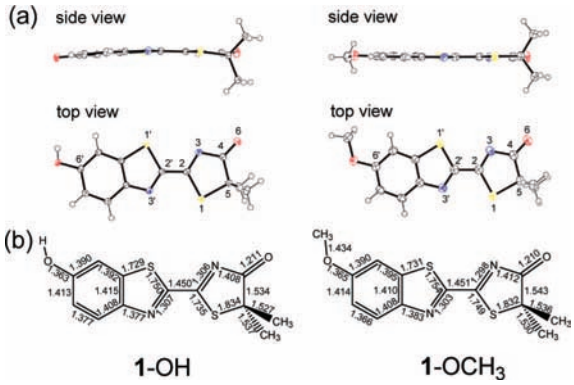

Figure 1. (a) Molecular structures of **1**-OH and **1**-OCH_3, with the atomic displacements drawn at the 50% probability level. (b) Selected bond distances (Å) are noted for **1**-OH and **1**-OCH_3.

of the mechanism to interpret the in vivo bioluminescence colors leads to a prediction of the properties of the active-site environment of firefly (beetle) luciferases.

Results and Discussion

Molecular Structures of 1-OH and 1-OCH_3. Compounds **1**-OH and **1**-OCH_3 were prepared by the modified method previously reported,[18,25,35] which is shown in the Experimental Section. The structures of **1**-OH and **1**-OCH_3 were confirmed by crystal structure analyses (Figure 1). In the crystals of **1**-OCH_3, two crystallographically independent molecules are present in the asymmetric unit, and their structures are similar to one another. Thus, one of the structures is shown in Figure 1. The structures of **1**-OH and **1**-OCH_3 in the crystals have the s-trans conformation and coplanarity of the thiazolone and benzothiazole rings. The molecular plane of **1**-OH is slightly bow-shaped. The s-trans planar conformation of **1**-OH is the same as that of OLH bound to a luciferase in a crystal.[16] The bond distances in **1**-OH and **1**-OCH_3 (Figure 1b) indicate a characteristic bond length alternation: the C2═N3 (1.30−1.31 Å) and C2′═N3′ (1.30−1.31 Å) bonds, for instance, have imine double-bond character, and the C4═O6 (1.21 Å) bond has carbonyl double-bond character. The C2−C2′ distances (1.45 Å) in **1**-OH and **1**-OCH_3 are the typical $C(sp^2)-C(sp^2)$ single bond length.

Spectroscopic Properties of 1-OH and 1-OCH_3. UV−vis absorption and fluorescence spectra of **1**-OH and **1**-OCH_3 were obtained in *p*-xylene, benzene, chloroform, DMSO, acetonitrile, 2-propanol, methanol, and H_2O. Spectra are shown in Figure 2, and the spectral data are summarized in Tables 1 and 2, where the data are listed in order of the solvent polarity scale $E_T(30)$ (in kcal mol^{-1}).[36] The data concerning the wavelengths of

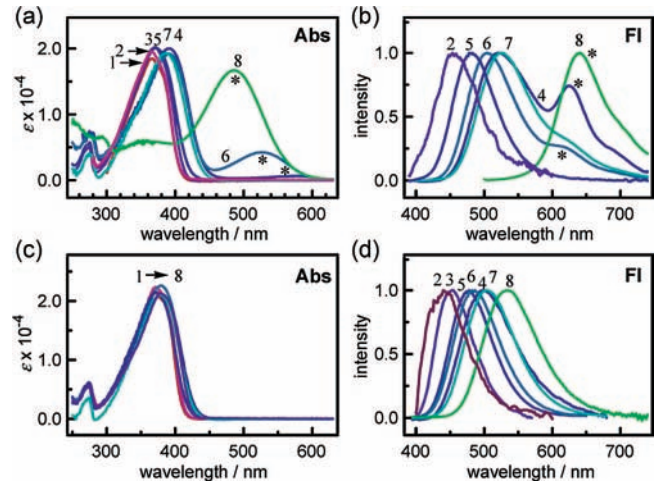

Figure 2. UV−vis absorption (Abs) and fluorescence (Fl) spectra of (a, b) **1**-OH and (c, d) **1**-OCH_3 in (1) *p*-xylene, (2) benzene, (3) chloroform, (4) DMSO, (5) acetonitrile, (6) 2-propanol, (7) methanol, and (8) H_2O at 25 °C. The asterisked absorption and emission bands in Figure 2a,b are due to the phenolate anion **1**-O^-.

UV−vis absorption and fluorescence emission maxima for **1**-OH in DMSO, methanol, and H_2O reproduce the values reported elsewhere within an allowance of ±5 nm.[19,29,32] The absorption spectra of **1**-OH and **1**-OCH_3 were similar to each other in *p*-xylene, benzene, chloroform, acetonitrile, and methanol (Figure 2a,c), while in 2-propanol and DMSO, a red-shifted absorption band of phenolate anion **1**-O^- accompanied the original one of **1**-OH. In water, the obtained absorption spectrum was due to **1**-O^- only. The methyl ether derivative **1**-OCH_3 showed decomposition in water, where its thiazolone ring may be hydrolyzed. While the absorption maxima of **1**-OH and **1**-OCH_3 were observed at 380 nm with a small solvent-dependent variation, their fluorescence emission maxima (λ_F) show a large variation depending on the solvent. The λ_F ranges of **1**-OH and **1**-OCH_3 are 420−526 and 440−535 nm, respectively, both of which have only a small overlap with the bioluminescence emission maxima (530−640 nm). These observations suggest that the neutral form of OLH is not the light-emitting species for the bioluminescence. Another characteristic of the fluorescence of **1**-OH and **1**-OCH_3 is the low quantum yield ($\Phi_F < 0.01$) in less polar solvents, such as *p*-xylene, benzene, and chloroform.

To evaluate the fluorescence spectral changes of **1**-OH and **1**-OCH_3 that depend on the solvent, we attempted to correlate the spectroscopic data with some solvent parameters. An analysis of the Stokes shifts with the Lippert−Mataga equation[37,38] did not give good correlations, indicating that solvent molecules affect the stability of the excited singlet states of **1**-OH and **1**-OCH_3 [^{1}(**1**-OH)* and ^{1}(**1**-OCH_3)*, respectively] by a specific interaction other than a simple dipole−dipole interaction. We also investigated correlations between $E_T(30)$ and the energy of the fluorescent state (E_F) estimated from λ_F. The solvent parameter $E_T(30)$ is employed for evaluating the ICT character of a molecule.[36] The E_F-versus-$E_T(30)$ plots (Figure 3) for **1**-OH and **1**-OCH_3 show linear correlations [$E_F = -0.49E_T(30) + 80$ ($r = -0.80$) for **1**-OH and $E_F = -0.38E_T(30) + 77$ ($r = -0.95$) for **1**-OCH_3], while the plots of the data in DMSO deviate from

(33) We have employed an approach of characterizing the excited molecule of the light emitter to explain the color modulation mechanism of jellyfish bioluminescence: (a) Hirano, T.; Mizoguchi, I.; Yamaguchi, M.; Chen, F. Q.; Ohashi, M.; Ohmiya, Y.; Tsuji, F. I. *Chem. Commun.* **1995**, 165–167. (b) Saito, R.; Hirano, T.; Niwa, H.; Ohashi, M. *Perkin Trans. 2* **1997**, 1711–1716. (c) Imai, Y.; Shibata, T.; Maki, S.; Niwa, H.; Ohashi, M.; Hirano, T. *J. Photochem. Photobiol., A* **2001**, *146*, 95–107. (d) Mori, K.; Maki, S.; Niwa, H.; Ikeda, H.; Hirano, T. *Tetrahedron* **2006**, *62*, 6272–6288.

(34) We presented some of the data in this paper at a meeting of the Chemical Society of Japan (CSJ) on March 29, 2008: Hasumi, Y.; Ohtsuka, K.; Kojima, S.; Maki, S.; Niwa, H.; Hirano, T. *Abstr. Pap.−Chem. Soc. Jpn.* **2008**, *88*, 1626.

(35) Suzuki, N.; Goto, T. *Agric. Biol. Chem.* **1972**, *36*, 2213–2221.

(36) Reichardt, C. In *Solvents and Solvent Effects in Organic Chemistry*, 3rd ed.; Wiley-VCH: Weinheim, Germany, 2003.

(37) Lippert, E. *Z. Electrochem.* **1957**, *61*, 962–975.

(38) Mataga, N.; Kaifu, Y.; Koizumi, M. *Bull. Chem. Soc. Jpn.* **1956**, *29*, 465–471.

Table 1. Electronic Absorption Data for **1**-OH and **1**-OCH_3 in Various Solvents in the Absence or Presence of Organic Bases (TBA, BA, TMG, and DBU) at 25 °C

	λ_{ab} (nm) [$\varepsilon/10^4$][b]		λ_{abs} (nm) [absorbance][c]			
solvent [$E_T(30)$[a]]	**1**-OCH_3	**1**-OH	**1**-OH + TBA[d]	**1**-OH + BA[d]	**1**-OH + TMG[d]	**1**-OH + DBU[d]
p-xylene [33.1]	368 [2.17]	366 [1.85]	377 [0.079]	−	500 sh[e] 401 [0.097]	−
benzene [34.3]	371 [2.24]	366 [1.95]	376 [0.080]	384 [0.080]	500 sh[e] 400 [0.088]	489 [0.040][e] 412 [0.071]
chloroform [39.1]	380 [2.12]	370 [2.04]	480 sh[e] 384 [0.084]	−	503 [0.019][e] 413 [0.021]	−
DMSO [45.1]	380 [2.11]	579 [0.06][e] 391 [2.00]	578 [0.025][e] 390 [0.088]	−	579 [0.257][e]	−
acetonitrile [45.6]	373 [2.14]	372 [2.01]	566 [0.012][e] 372 [0.070]	564 [0.016][e]	565 [0.116][e]	564 [0.106][e]
2-propanol [48.4]	380 [2.26]	526 [0.42][e] 391 [1.92]	525 [0.006][e] 390 [0.102]	−	527 [0.158][e]	−
methanol [55.4]	378 [2.11]	388 [1.93]	485 [0.079][e]	−	484 [0.079][e]	−
water [63.1]	~380 [n.d.][f]	486 [1.67][e]	−	−	484 [n.d.][e,f]	−

[a] $E_T(30)$ in kcal mol^{-1}. [b] Extinction coefficient in dm^3 mol^{-1} cm^{-1}. [c] Concentration of **1**-OH was 5.0×10^{-6} mol dm^{-3}. [d] Concentrations of the organic bases were 0.010 mol dm^{-3}. Abbreviations: TBA, tributylamine; BA, butylamine; TMG, 1,1,3,3-tetramethylguanidine; DBU, 1,8-diazabicyclo[5.4.0]undec-7-ene. [e] Absorption maxima of the phenolate anion **1**-O^-. See the text for details. [f] Not determined accurately because of decomposition of the substrate.

Table 2. Fluorescence of **1**-OCH_3, **1**-OH, and **1**-O^- in Various Solvents at 25 °C

	λ_F (nm) [Φ_F]					
solvent [$E_T(30)$[a]]	**1**-OCH_3[b]	**1**-OH[b]	**1**-O^-/H-TBA$^+$ [c]	**1**-O^-/H-BA$^+$ [c]	**1**-O^-/H-TMG$^+$ [c]	**1**-O^-/H-DBU$^+$[c]
p-xylene [33.1]	weak	~420[d]	541 [0.46]	−	563 [0.25]	−
benzene [34.3]	440[d]	~420[d]	541 [0.82]	547 [0.50]	570 [0.25]	566 [0.45]
chloroform [39.1]	454 [0.002]	454 [0.001]	588 [0.75]	−	601 [0.53]	−
DMSO [45.1]	499 [0.008]	522 [0.07][e]	630 [0.53]	−	631 [0.51]	−
acetonitrile [45.6]	478 [0.02]	479 [0.03]	624 [0.26]	624 [0.23]	624 [0.22]	624 [0.22]
2-propanol [48.4]	487 [0.02]	504 [0.11][e]	624 [0.29]	−	624 [0.27]	−
methanol [55.4]	505 [0.12]	526 [0.19]	630 [0.08]	−	630 [0.10]	−
water [63.1]	535 [n.d.][g]	640 [0.04][f]	−	−	637 [n.d.][g]	−

[a] $E_T(30)$ in kcal mol^{-1}. [b] Concentrations of **1**-OH and **1**-OCH_3 were 1.0×10^{-6} mol dm^{-3}. [c] Initial concentrations of **1**-OH and organic bases were 5.0×10^{-6} and 0.010 mol dm^{-3}, respectively. [d] Quantum yield Φ_F was lower than 0.001. [e] Excitation wavelength was 380 nm. [f] Fluorescence of the phenolate anion **1**-O^-. [g] Not determined accurately because of decomposition of the substrate.

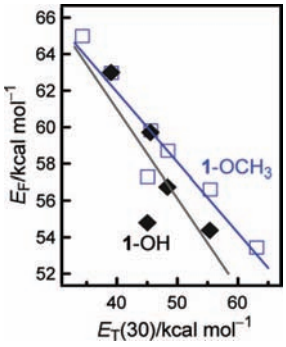

Figure 3. E_F values for **1**-OH (◆) and **1**-OCH_3 (□) plotted as functions of $E_T(30)$.

linearity. The data thus obtained were compared with those for compounds whose excited singlet states have ICT character, such as 2-(*N*-phenylamino)-6-naphthalenesulfonate (ANS)[39] and *Cypridina* oxyluciferin analogue [2-acetamido-5-(3-indolyl)pyrazine].[40] The slopes of the $E_F-E_T(30)$ correlations for **1**-OH and **1**-OCH_3 are smaller than that of the $E_F-E_T(30)$ correlation for ANS [$E_F = -0.55E_T(30) + 95$ ($r = -0.99$)][39] but similar to that of the $E_F-E_T(30)$ correlation for *Cypridina* oxyluciferin analogue [$E_F = -0.43E_T(30) + 84$ ($r = -0.97$)].[40] Therefore, ^{1}(**1**-OH)* and ^{1}(**1**-OCH_3)* also have ICT character, which is weaker than that of the excited singlet state of ANS and similar to that of the excited singlet state of *Cypridina* oxyluciferin analogue.

Spectroscopic Properties of Phenolate Anion 1-O^-. Spectroscopic measurements of **1**-OH in 2-propanol, DMSO, and water showed the generation of **1**-O^- in the absence of bases. To investigate the spectroscopic properties of **1**-O^-, spectroscopic measurements were carried out in the presence of the organic bases tributylamine (TBA), butylamine (BA), 1,1,3,3-tetramethylguanidine (TMG), and 1,8-diazabicyclo[5.4.0]undec-7-ene (DBU). Conjugate acids of these organic bases (i.e., H-TBA$^+$, H-BA$^+$, H-TMG$^+$, and H-DBU$^+$) behave as countercations for **1**-O^-. UV−vis absorption and fluorescence spectra of **1**-OH in benzene and acetonitrile containing these organic bases are shown in Figure 4, and the spectral data are summarized in Tables 1 and 2.

Spectral changes in the UV−vis absorption of **1**-OH in the presence of an organic base indicate formation of a hydrogen-bonded complex (HBC) of **1**-OH with the base (N[base]) and/or generation of **1**-O^- with the conjugate acid of the organic base (HN[base]$^+$) (Scheme 2).[33,41,42] No spectral changes were

(39) (a) Kosower, E. M.; Tanizawa, K. *Chem. Phys. Lett.* **1972**, *16*, 419–425. (b) Kosower, E. M.; Dodiuk, H.; Tanizawa, K.; Ottolenghi, M.; Orbach, N. *J. Am. Chem. Soc.* **1975**, *97*, 2167–2178.
(40) Hirano, T.; Takahashi, Y.; Kondo, H.; Maki, S.; Kojima, S.; Ikeda, H.; Niwa, H. *Photochem. Photobiol. Sci.* **2008**, *7*, 197–207.
(41) Laurence, C.; Berthelot, M.; Graton, J. *The Chemistry of Phenols, Part 1*; Rappoport, Z., Ed.; Wiley: Chichester, U.K., 2003; pp 529−603.
(42) Pines, E. *The Chemistry of Phenols, Part 1*; Rappoport, Z., Ed.; Wiley: Chichester, U.K., 2003; pp 491−527.

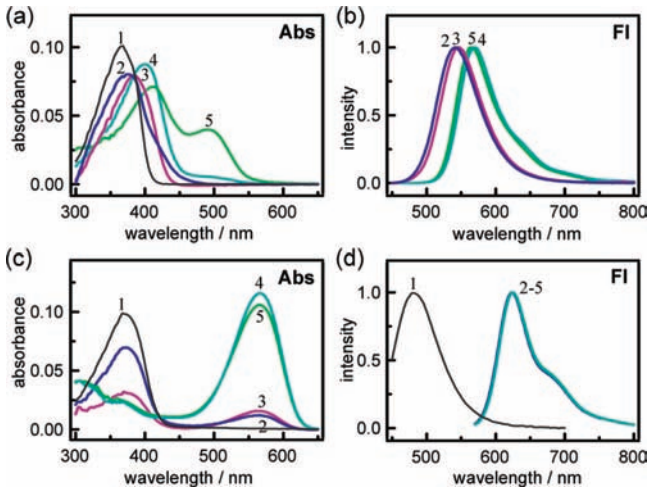

Figure 4. UV−vis absorption (Abs) and fluorescence (Fl) spectra of **1**-OH (5.0×10^{-6} mol dm^{-3}) in (a, b) benzene and (c, d) acetonitrile containing the following organic bases (0.010 mol dm^{-3}): (1) no base, (2) TBA, (3) BA, (4) TMG, and (5) DBU at 25 °C.

seen for **1**-OCH$_3$ in the presence of these organic bases. In benzene (Figure 4a), addition of TBA or BA resulted in the appearance of a small red-shifted band at ∼400 nm, indicating the formation of an HBC of **1**-OH and N[base]. In contrast, addition of TMG or DBU in benzene resulted in the appearance of a large red-shifted band at ∼500 nm, indicating generation of **1**-O$^-$ in an ion pair with HN[base]$^+$. Additions of the four organic bases to acetonitrile solutions of **1**-OH resulted in the appearance of large red-shifted bands at 565 nm irrespective of N[base] (Figure 4c). These results indicate the predominant generation of **1**-O$^-$ with HN[base]$^+$ in polar solvents.

Fluorescence of **1**-O$^-$ was observed upon excitation of **1**-OH in an HBC with N[base] as well as upon excitation of **1**-O$^-$ (Figure 4b,d). In benzene containing TBA or BA, the fluorescence emission maximum λ_F of **1**-O$^-$ showed a large Stokes shift (∼8000 cm^{-1}). This result indicates that ^{1}(**1**-OH)* in an HBC with TBA or BA gives the excited singlet state of **1**-O$^-$ [^{1}(**1**-O$^-$)*] in an ion pair with H-TBA$^+$ or H-BA$^+$, respectively, by proton transfer, as shown in Scheme 2a; this is a well-known mechanism for fluorescence emission of a phenol derivative making an HBC with an organic base in a less polar solvent.[33,43−45] In contrast, the fluorescence spectrum of **1**-O$^-$ in benzene containing TMG or DBU showed a mirror image of the corresponding absorption spectrum with a small Stokes shift (∼2600 cm^{-1}), indicating that fluorescence emission takes place from ^{1}(**1**-O$^-$)* generated by direct electronic excitation of **1**-O$^-$ in an ion pair (Scheme 2b). The observation that the λ_F value of **1**-O$^-$ in benzene depends on HN[base]$^+$ indicates that a contact ion pair (CIP) of ^{1}(**1**-O$^-$)* and HN[base]$^+$ is formed in a less polar solvent (Scheme 2a,b)[36,46] and that the fluorescence properties of **1**-O$^-$ are affected by the strength of the bonding interaction with HN[base]$^+$. The degree of the red shift of λ_F is in the order TMG > DBU > BA > TBA. This order may correspond to that of the acidities (pK_a) of HN[base]$^+$, whose values were reported to be 23.3, 24.1, 18.3, and 18.1 in acetonitrile for H-TMG$^+$, H-DBU$^+$, H-BA$^+$, and H-TBA$^+$, respectively,[47,48] although the order of the pK_a values for H-TMG$^+$ and H-DBU$^+$ is opposite. Therefore, with an increase in the acidity of HN[base]$^+$, the anionic character of ^{1}(**1**-O$^-$)* in a CIP with HN[base]$^+$ decreases, and the λ_F value shifts toward the blue region. In contrast, fluorescence spectra of **1**-O$^-$ in acetonitrile were not affected by HN[base]$^+$, indicating that ^{1}(**1**-O$^-$)* is present as the counteranion of a solvent-separated ion pair (SSIP) or a free ion couple with HN[base]$^+$ in a polar solvent (Scheme 2c).[36,46] The interaction between ^{1}(**1**-O$^-$)* and HN[base]$^+$ may be too weak to change the λ_F value. The fluorescence quantum yields of **1**-O$^-$ in benzene and acetonitrile were estimated to be in the range from 0.22 to 0.82. The Φ_F values may be modulated by the strength of the interaction between ^{1}(**1**-O$^-$)* and HN[base]$^+$, but a tendency in their change is not very apparent.

To evaluate the solvent effect on the emission from ^{1}(**1**-O$^-$)*, fluorescence spectra of **1**-O$^-$ were measured in various solvents containing TBA or TMG (Figure 5). The λ_F value (637 nm) of **1**-O$^-$ in water containing TMG is slightly different from that (640 nm) observed in water in the absence of bases, suggesting that the presence of TMG slightly induces a polarity change in the aqueous solution. In water/TMG, decomposition of **1**-O$^-$ was observed, as reported previously.[32a] The λ_F values of **1**-O$^-$ in methanol, 2-propanol, acetonitrile, and DMSO are in the range 624−630 nm and are not affected by the identity of HN[base]$^+$. These facts indicate that ^{1}(**1**-O$^-$)* exists as the counteranion in an SSIP or a free ion couple with HN[base]$^+$. Thus, the variation of the λ_F values is due to the effect of the solvent polarity on the properties of ^{1}(**1**-O$^-$)*. Conversely, in chloroform, benzene, and *p*-xylene, the λ_F values of **1**-O$^-$ showed a dependence on HN[base]$^+$, indicating that **1**-O$^-$ forms a CIP with HN[base]$^+$ and that the properties of ^{1}(**1**-O$^-$)* are affected by a bonding interaction between ^{1}(**1**-O$^-$)* and HN[base]$^+$ together with the solvent polarity.

The solvent-dependent variation of the λ_F values for **1**-O$^-$ was evaluated by correlating the E_F values estimated from λ_F with the solvent parameter $E_T(30)$.[36] The E_F-versus-$E_T(30)$ plots (Figure 6) can be divided into two groups, one in the $E_T(30)$ range from 45 to 63 for polar solvents (DMSO, acetonitrile, 2-propanol, methanol, and water) and the other in the $E_T(30)$ range from 33 to 45 for less polar solvents (*p*-xylene, benzene, chloroform, and DMSO). In each group, the plots show straight lines with respect to $E_T(30)$. One line for the plots in the polar-solvent region [$E_T(30) = 45-63$] is represented by the equation $E_F = -0.05E_T(30) + 48.0$ ($r = -0.81$) irrespective of HN[base]$^+$. In the plots for less polar solvents [$E_T(30) = 33-45$], two lines can be seen: $E_F = -0.66E_T(30) + 75$ ($r = -0.99$) for **1**-O$^-$/H-TBA$^+$ and $E_F = -0.46E_T(30) + 66$ ($r = -0.99$) for **1**-O$^-$/H-TMG$^+$. The data point for the E_F value in DMSO at $E_T(30) = 45$ happens to be located at the crossing of these three lines. In the $E_T(30) = 33-45$ region, the slopes are clearly different from each other, indicating that the bonding interaction between ^{1}(**1**-O$^-$)* and H-TBA$^+$ has a different strength from that between ^{1}(**1**-O$^-$)* and H-TMG$^+$. These bonding interactions influence the π-electron properties of ^{1}(**1**-O$^-$)*, resulting in a variation of the λ_F values. The plot for **1**-O$^-$/H-TBA$^+$ shows a steeper slope than that for **1**-O$^-$/H-TMG$^+$. This result corresponds to the difference in the acidities: the

(43) Matsuzaki, A.; Nagakura, S.; Yoshihara, K. *Bull. Chem. Soc. Jpn.* **1974**, *47*, 1152–1157.
(44) Tolbert, L. M.; Nesselroth, S. M. *J. Phys. Chem.* **1991**, *95*, 10331–10336.
(45) Willis, K. J.; Szabo, A. G. *J. Phys. Chem.* **1991**, *95*, 1585–1589.
(46) *Ions and Ion Pairs in Organic Reactions*; Szwarc, M., Ed.; Wiley-Interscience: New York, 1972; Vol. 1.
(47) Kolthoff, I. M.; Chantooni, M. K., Jr.; Bhowmik, S. *J. Am. Chem. Soc.* **1968**, *90*, 23–28.
(48) Galezowski, W.; Jarczewski, A.; Stanczyk, M.; Brzezinski, B.; Bartl, F.; Zundel, G. *J. Chem. Soc., Faraday Trans.* **1997**, *93*, 2515–2518.

Scheme 2

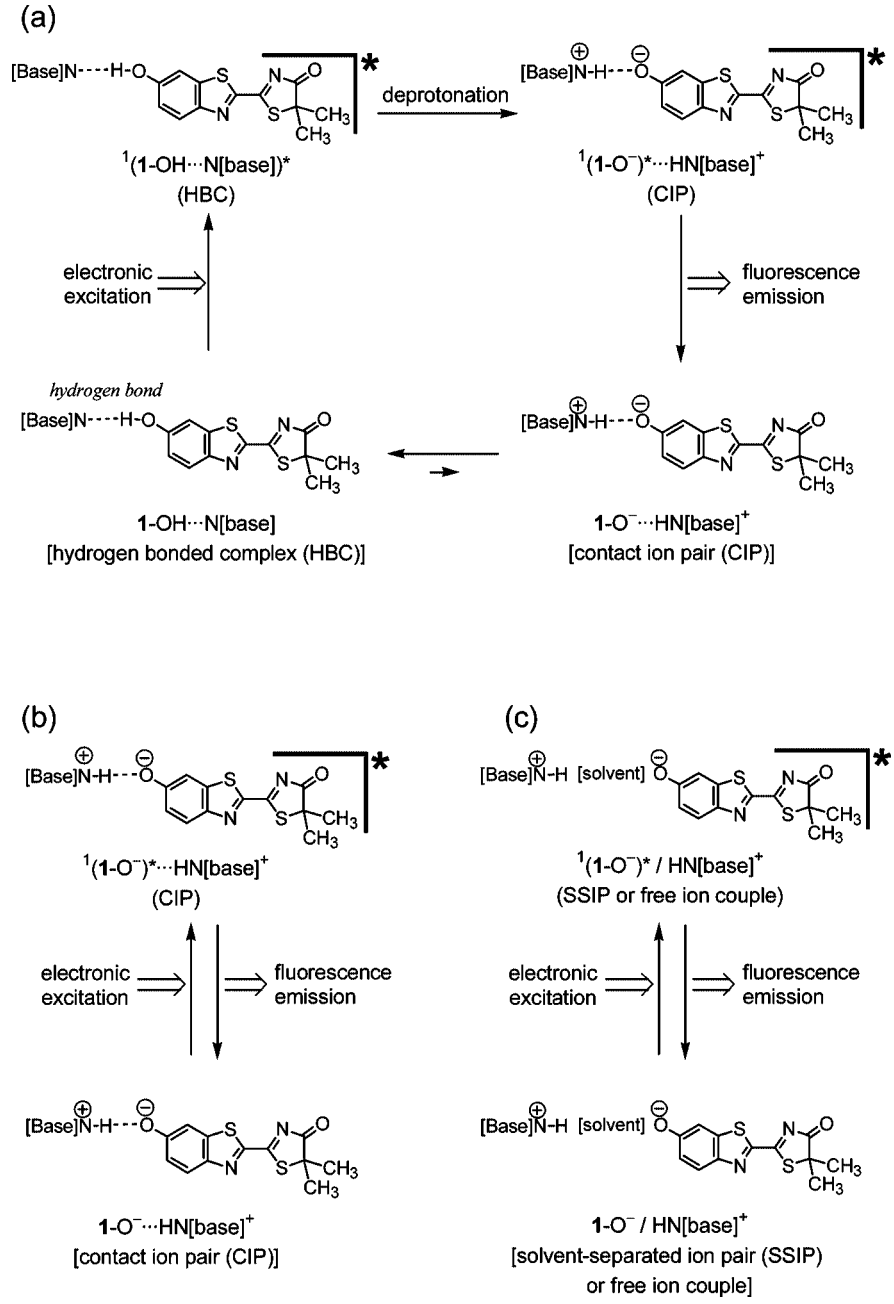

acidity of H-TBA$^+$ is stronger than that of H-TMG$^+$.[47] Therefore, an increase in the acidity of HN[base]$^+$ is favorable for widely modulating the strength of the bonding interaction between ^{1}(**1**-O$^-$)* and HN[base]$^+$, resulting in an expansion of the range of variable λ_F values.

Fluorescence Lifetime Measurements. To investigate the properties of ^{1}(**1**-O$^-$)* under representative base/solvent combinations, we determined the fluorescence lifetimes (τ_F) of **1**-O$^-$ and **1**-OH in benzene and acetonitrile using a time-correlated single-photon counting method (Table 3). In the presence of the organic bases (TBA, BA, TMG, and DBU) in the solutions of **1**-OH, the fluorescence decay curves were fitted with two exponential decay components. The minor component ($\leq$9%) showed a variation of τ_F values (5−10 ns) depending on the solvent and base that differed from that of the major component. This result suggests that the minor component is caused by emission from the excited states of the chemical species whose structures are not similar to that for the major component. Thus, the compound for the minor component is not a conformational isomer of that for the major component but presumably a byproduct generated from **1**-OH under basic conditions. Therefore, the major component can be due to the decay of the emission from ^{1}(**1**-O$^-$)*. That is, the lifetime for the major component is the intrinsic one for fluorescence from ^{1}(**1**-O$^-$)*. The τ_F values for ^{1}(**1**-O$^-$)* are larger than those of the neutral form **1**-OH (τ_F < 0.5 ns). Interestingly, the τ_F values of **1**-O$^-$ in benzene were found to depend on the countercations (HN[base]$^+$), while those in acetonitrile are identical (τ_F = 1.9 ns).

Quantum-Chemical Calculations. In order to understand the spectroscopic properties of **1**-OH and **1**-O$^-$, we carried out density functional theory (DFT) calculations on **1**-OH, **1**-OCH$_3$, **1**-O$^-$, and an ion pair of **1**-O$^-$ with a countercation as well as

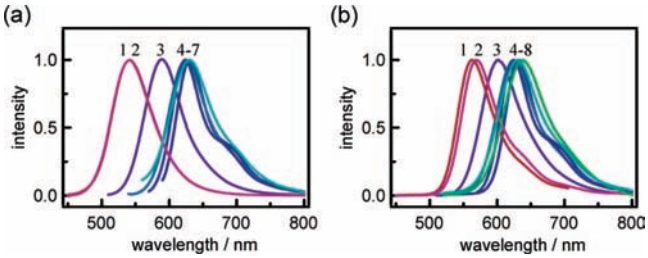

Figure 5. Fluorescence spectra of **1**-OH (5.0×10^{-6} mol dm^{-3}) in the presence of (a) TBA (0.010 mol dm^{-3}) and (b) TMG (0.010 mol dm^{-3}) in (1) *p*-xylene, (2) benzene, (3) chloroform, (4) DMSO, (5) acetonitrile, (6) 2-propanol, (7) methanol, and (8) H_2O at 25 °C.

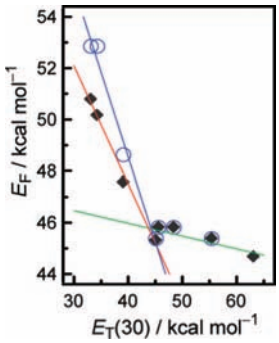

Figure 6. E_F values for **1**-O$^-$/TBA-H$^+$ (○) and **1**-O$^-$/TMG-H$^+$ (◆) plotted as functions of $E_T(30)$.

Table 3. Fluorescence Lifetimes (τ_F) of **1**-OH and **1**-O$^-$ in Benzene and Acetonitrile at 25 °C

solvent	base[a]	λ_{ex} (nm)[b]	λ_{em} (nm)[c]	τ_F (ns) [weight[d]]
benzene	none	360	415	<0.5
	TBA	376	541	3.3 [96%], 8.4 [4%]
	BA	384	547	2.4 [98%], 10.0 [2%]
	TMG	400	570	0.83 [97%], 7.0 [3%]
	DBU	412	566	1.3 [98%], 8.0 [2%]
acetonitrile	none	373	479	<0.5
	TBA	565	630	1.9 [91%], 5.1 [9%]
	BA	564	624	1.9 [95%], 6.7 [5%]
	TMG	565	630	1.9 [93%], 6.0 [7%]
	DBU	564	624	1.9 [95%], 7.3 [5%]

[a] When base was present, its concentration was 0.010 mol dm^{-3}. [b] Excitation wavelength. [c] Monitored emission wavelength. [d] Weight of the component in the double-exponential fit.

on OLH and OL$^-$ [49] at the B3LYP/6-31+G(d) level.[50−53] We optimized the geometries of the s-cis and s-trans conformers for these compounds. To eliminate the complexity of using HN[base]$^+$ (e.g., H-TBA$^+$ or H-TMG$^+$) for calculations of ion pairs, we employed the alkaline metal ions Li^+, Na^+, and K^+ as countercations for ion pairs with **1**-O$^-$ (Chart 1). The calculated data are summarized in Table 4. It was confirmed that the calculated data for OLH and OL$^-$ reproduced the reported data.[49] All of the s-cis and s-trans conformers were optimized as coplanar structures of the two ring systems. The values of ΔE_{t-c}, the heat of formation of the s-trans conformer relative to the corresponding s-cis conformer, indicate that the

Chart 1

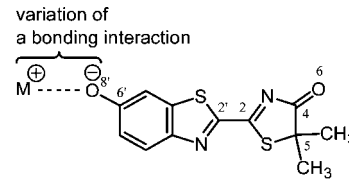

1-O$^-$M$^+$
(M$^+$ = Li$^+$, Na$^+$, K$^+$)

Table 4. Relative Energies (ΔE_{t-c}) of the S-Cis and S-Trans Conformers and Bond Distances and Mulliken Charge Densities (q) for the Benzothiazole (BT) and Thiazolone (TA) Moieties of the S-Trans Conformers of Oxyluciferin and Its Derivatives in the Gas Phase, Obtained Using DFT at the B3LYP/6-31+G(d) Level

		bond distances (Å)					
compound	ΔE_{t-c} (kcal mol^{-1})[a]	C2−C2′	C4═O6	C6′−O8′	O8′−M	q_{BT}[b]	q_{TA}[c]
OLH	−6.21	1.455	1.212	1.366	−	0.059	−0.059
OL$^-$	−5.47	1.413	1.227	1.257	−	−0.653	−0.347
1-OH	−6.06	1.457	1.214	1.367	−	0.039	−0.039
1-OCH$_3$	−5.45	1.457	1.215	1.362	−	0.067	−0.067
1-O$^-$	−5.44	1.413	1.229	1.257	−	−0.665	−0.336
1-O$^-$Li$^+$	−6.01	1.447	1.217	1.313	1.635	0.139	−0.139
1-O$^-$Na$^+$	−5.94	1.443	1.218	1.303	1.999	0.153	−0.153
1-O$^-$K$^+$	−5.92	1.440	1.219	1.298	2.343	0.177	−0.177

[a] Energy of an s-trans conformer relative to that of the corresponding s-cis conformer. [b] Mulliken charge density of the benzothiazole moiety including a substituent. [c] Mulliken charge density of the thiazolone moiety.

s-trans conformer is the energetically favorable structure. The optimized structures of **1**-OH and **1**-OCH$_3$ are similar to that of OLH, while that of **1**-O$^-$ is similar to that of OL$^-$.[49] The neutral molecules OLH, **1**-OH, and **1**-OCH$_3$ have C2−C2′ and C6′−O8′ bonds with typical C(sp^2)−C(sp^2) and C(sp^2)−O(sp^3) single-bond characters, respectively, and C4═O6 bonds with typical carbonyl double-bond character. The geometries of the s-trans conformers of **1**-OH and **1**-OCH$_3$ obtained from the computations agree well with those of **1**-OH and **1**-OCH$_3$ determined by crystal structure analyses. The Mulliken charge densities of the benzothiazole and thiazolone moieties (q_{BT} and q_{TA}, respectively) are slightly positive and negative, respectively, in OLH, **1**-OH, and **1**-OCH$_3$, indicating that the ground states of these molecules are weakly polarized. The negative charges of OL$^-$ and **1**-O$^-$ are delocalized to the benzothiazole and thiazolone moieties by π-electron conjugation. Therefore, the double-bond character of the C2−C2′ and C6′−O8′ bonds of OL$^-$ and **1**-O$^-$ increases, and the single-bond character of the C4═O6 bonds increases. The structural characteristics of **1**-O$^-$M$^+$ are intermediate between those of **1**-OH and **1**-O$^-$ and vary depending on the identity of M$^+$. The degree of ionic character of the O8′−M bond in **1**-O$^-$M$^+$ can be expressed in terms of the Mulliken charge densities of M$^+$, which are +0.93 (K$^+$), +0.91 (Na$^+$), and +0.56 (Li$^+$). This degree corresponds to the strength of the anionic character of the **1**-O$^-$ moiety in **1**-O$^-$M$^+$, while it is inversely proportional to the degree of covalent character of the O8′−M bond. The results obtained from the DFT calculations indicate that the properties of **1**-O$^-$ are modulated by a bonding interaction with a countercation.

Next we investigated the properties of gas-phase electronic excitations of **1**-OH, **1**-OCH$_3$, **1**-O$^-$, and **1**-O$^-$M$^+$ and of OLH and OL$^-$ [49] by time-dependent DFT (TDDFT) calculations at the B3LYP/6-31+G(d) level.[50−53] Table 5 summarizes the data for their electric-dipole-allowed transitions to the excited singlet

(49) Orlova, G.; Goddard, J. D.; Brovko, L. Y. *J. Am. Chem. Soc.* **2003**, *125*, 6962–6971.
(50) Frisch, M. J.; et al. *Gaussian 03*, revision C.02; Gaussian, Inc.: Wallingford, CT, 2004.
(51) Becke, A. D. *J. Chem. Phys.* **1993**, *98*, 5648–5652.
(52) Lee, C.; Yang, W.; Parr, R. G. *Phys. Rev. B* **1988**, *37*, 785–789.
(53) Stephens, P. J.; Devlin, F. J.; Chabalowski, C. F.; Frisch, M. J. *J. Phys. Chem.* **1994**, *98*, 11623–11627.

Table 5. Vertical Excitation Energies (E_{ex}), Excitation Wavelengths (λ_{ex}), Oscillator Strengths (f), and Configurations Predicted for the Allowed Transitions to the Excited Singlet States with the Lowest Excitation Energies for the S-Trans Conformers of Oxyluciferin and Its Derivatives, Obtained Using TDDFT at the B3LYP/6-31+G(d) Level

compound	transition	E_{ex} (eV)	λ_{ex} (nm)[a]	f	configuration[b]
OLH [c]	$S_0 \rightarrow S_1$	3.32	374	0.29	H → L (0.62), H−1 → L (0.22)
OL^- [c]	$S_0 \rightarrow S_1$	2.54	488	0.64	H → L (0.56), H−2 → L (0.17)
1-OH	$S_0 \rightarrow S_2$	3.33	373	0.32	H → L (0.62), H−1 → L (0.22)
1-OCH_3	$S_0 \rightarrow S_1$	3.22	385	0.34	H → L (0.63), H−1 → L (0.18)
1-O^-	$S_0 \rightarrow S_1$	2.53	491	0.68	H → L (0.56), H−2 → L (−0.17)
1-O^-Li^+	$S_0 \rightarrow S_2$	2.91	426	0.54	H → L (0.63), H−1 → L (0.13)
1-O^-Na^+	$S_0 \rightarrow S_2$	2.79	444	0.56	H → L+1 (0.62), H−1 → L+1 (−0.13)
1-O^-K^+	$S_0 \rightarrow S_2$	2.74	453	0.58	H → L+1 (0.61), H−1 → L+1 (−0.13)

[a] Excitation wavelengths estimated from the corresponding E_{ex} values. [b] Configuration of the excitation: H, H−n, L, and L+1 denote the HOMO, HOMO−n, LUMO, and LUMO+1, respectively. [c] Data from ref 49.

states with the lowest excitation energies.[49] The transitions $S_0 \rightarrow S_1$ and $S_0 \rightarrow S_2$, respectively, correspond to HOMO → LUMO excitations for OLH, OL^-, **1**-OH, **1**-OCH_3, **1**-O^-, and **1**-O^-Li^+ and to HOMO → LUMO+1 excitations for **1**-O^-Na^+ and **1**-O^-K^+. The plots of the Kohn−Sham frontier orbitals of **1**-OH, **1**-OCH_3, **1**-O^-, and **1**-O^-M^+ indicate that these allowed transitions are of the $\pi \rightarrow \pi^*$ type. All of the π^* orbitals have π-bonding character between C2 and C2′, indicating that the lowest excited singlet states maintain coplanar structures of the two rings.[49,54] The excitation wavelengths (λ_{ex}) for the allowed lowest-energy transitions of OL^- (488 nm) and **1**-O^- (491 nm) are similar to each other. This result indicates that the two methyl groups in **1**-O^- influence to a lesser extent the properties of the π-electron system. The λ_{ex} values of **1**-OH (373 nm) and **1**-OCH_3 (385 nm) agree with the observed absorption maxima in benzene (**1**-OH, 366 nm; **1**-OCH_3, 371 nm). The λ_{ex} value (491 nm) of free **1**-O^- is close to the observed absorption maximum in water (486 nm), while the absorption maxima of **1**-O^- vary depending on both the ion-pair properties and the solvent polarity. The λ_{ex} values of **1**-O^-M^+ are intermediate between those of **1**-OH and free **1**-O^-. The variation of λ_{ex} depends on the degree of ionic character of the O8′−M bond in **1**-O^-M^+. A decrease in ionic character (an increase in covalent character) of the O8′−M bond in **1**-O^-M^+ causes a blue shift in λ_{ex}.

Relationship between the Fluorescence Properties of 1-O^- and Ion-Pair Structures. The results obtained in the present work give useful information to make clear the relationship between the fluorescent properties of **1**-O^- and ion-pair structures. We observed that the fluorescence spectra of **1**-O^- in a polar solvent such as acetonitrile were not influenced by the identity of HN[base]$^+$. From this result, it is inferred that ^{1}(**1**-O^-)* is present as the counteranion in an SSIP or a free ion couple with HN[base]$^+$ in a polar solvent (Scheme 2c). In contrast, the λ_F value of **1**-O^- in a less polar solvent such as benzene depends on HN[base]$^+$. This result indicates that a CIP of ^{1}(**1**-O^-)* and HN[base]$^+$ is formed (Schemes 2a,b). These emission properties of ^{1}(**1**-O^-)* that depend on the solvent polarity and the ion-pair structures are consistent with those obtained from the analyses of the E_F-versus-E_T(30) plots (Figure 6) and the fluorescence lifetimes of **1**-O^- (Table 3). The E_F-versus-E_T(30) plots for **1**-O^-/H-TBA$^+$ and **1**-O^-/H-TMG$^+$ in the polar-solvent region [E_T(30) = 45−63] gave one line irrespective of HN[base]$^+$. Similarly, the fluorescence lifetimes (τ_F) of **1**-O^- in acetonitrile were constant irrespective of HN[base]$^+$. These results indicate that ^{1}(**1**-O^-)* is present as a counteranion in an SSIP or a free ion couple with HN[base]$^+$. In this case, the emission properties of ^{1}(**1**-O^-)* are not affected by the identity of HN[base]$^+$ but only by the solvent polarity. The small values of the slopes of the E_F-versus-E_T(30) plots indicate that the λ_F value for the emission from ^{1}(**1**-O^-)* has a small dependence on the solvent polarity. In contrast, the E_F-versus-E_T(30) plots for **1**-O^-/H-TBA$^+$ and **1**-O^-/H-TMG$^+$ in less polar solvents [E_T(30) = 33−45] gave lines that differed from one another. In addition, the τ_F values of **1**-O^- in benzene varied depending on the identity of HN[base]$^+$. These findings indicate that ^{1}(**1**-O^-)* and HN[base]$^+$ make a CIP and that the emission properties of ^{1}(**1**-O^-)* are affected by a bonding interaction between ^{1}(**1**-O^-)* and HN[base]$^+$. Because the E_F-versus-E_T(30) plots in the less polar region show two types of line, the bonding interaction between ^{1}(**1**-O^-)* and HN[base]$^+$ is operative in the solvent dependence of the pertinent emission-color variation. It is reported that the acidity of H-TBA$^+$ (pK_a = 18.1) is greater than that of H-TMG$^+$ (pK_a = 23.3).[47] The observation that the slope of the plot for **1**-O^-/H-TBA$^+$ is greater than that for **1**-O^-/H-TMG$^+$ indicates that an increase in the acidity of HN[base]$^+$ causes an expansion of the strength range of the bonding interaction between ^{1}(**1**-O^-)* and HN[base]$^+$, which results in a wider range of variable λ_F values.

To understand the characteristics of the bonding interaction between ^{1}(**1**-O^-)* and HN[base]$^+$ in a CIP, we evaluated the λ_F values of **1**-O^- using results of the DFT calculations. The theoretical studies of OL^- and its related structures reported previously[49,54] indicate that the variation of their λ_F values is closely related to that of their corresponding absorption wavelengths (λ_{ex}). Thus, we scrutinized the relationship between the observed λ_F values of **1**-O^- and the λ_{ex} values calculated for the ion-pair models **1**-O^-M^+ and free **1**-O^-. We found that the λ_F value shifts toward the blue region with decreasing anionic character of ^{1}(**1**-O^-)* in a CIP with HN[base]$^+$ in a less polar solvent (Scheme 3). The experimental results agree with the calculated ones in that the λ_{ex} value for **1**-O^-M^+ shifts toward the blue region with a decrease in the ionic character of the O8′−M bond. The decrease in the ionic character of the O8′−M bond corresponds to an increase in its covalent character. Therefore, an increase in the covalent character of the O8′···H bond in the ion pair of ^{1}(**1**-O^-)* with HN[base]$^+$ weakens the phenolate ion character of ^{1}(**1**-O^-)*, resulting in a blue shift of the λ_F value. We also found that λ_F of **1**-O^- in a CIP in a less polar solvent is shorter than those in an SSIP or a free ion couple in a polar solvent. This observation is supported by the calculated result that λ_{ex} of **1**-O^-M^+ is shorter than that of free **1**-O^-.

Scheme 3

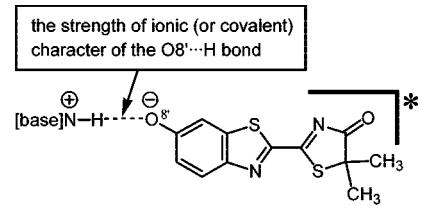

contact ion pair of ^{1}(**1**-O^-)* and HN[base]$^+$

(54) (a) Ren, A.-M.; Goddard, J. D. *J. Photochem. Photobiol., B* **2005**, *81*, 163–170. (b) Yang, T.; Goddard, J. D. *J. Phys. Chem. A* **2007**, *111*, 4489–4497.

Scheme 4

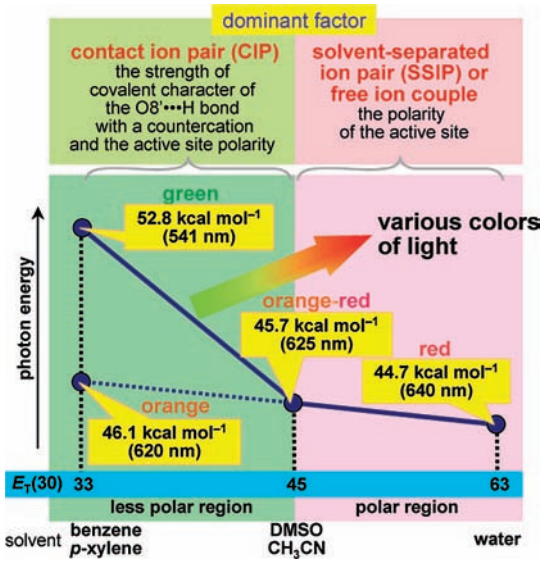

Light-Color Modulation Mechanism of Firefly (Beetle) Bioluminescence. In the present study, we have shown that the fluorescent properties of **1**-O^- are modulated by both the solvent polarity and the bonding interaction between ^{1}(**1**-O^-)* and HN[base]$^+$. Although **1**-O^- has two extra methyl groups at C5 compared with OL^-, these methyl groups should have little effect on the emission properties of ^{1}(**1**-O^-)*. This prediction is supported by the DFT calculations, which indicate that the π-electron properties of OL^- and **1**-O^- are similar to each other. Thus, it is reasonable to consider the emission properties of $^1(OL^-)$* using those of ^{1}(**1**-O^-)* for the light-color modulation mechanism of the firefly (beetle) bioluminescence. The bioluminescence emission maximum appears in the 530−640 nm wavelength region.[7−9] We have shown that the fluorescence emission maximum of **1**-O^- is in the range 541−640 nm, which covers almost the whole range of the bioluminescence emission maximum. Therefore, we can explain the mechanism of the multicolor bioluminescence by considering only one species in the excited singlet state, namely, $^1(OL^-)$*. We propose here the following light-color modulation mechanism: (1) the light emitter is the excited singlet state of the keto form of oxyluciferin phenolate anion, $^1(OL^-)$*, and (2) the emission maximum of OL^- is modulated by two main factors: the polarity of the active-site environment of the luciferase surrounding $^1(OL^-)$* and the properties of the bonding interaction between the O8′ atom of $^1(OL^-)$* and a hydrogen atom of a countercation, which will be the protonated form of a basic moiety of an amino acid residue in the active site. The influence of these two factors on the emission maximum of OL^- can be quantitatively predicted on the basis of the results of the E_F-versus-E_T(30) plot analyses for the **1**-O^-/H-TBA$^+$ and **1**-O^-/H-TMG$^+$ systems, as shown in Scheme 4. The solid line of the correlation between photon energy (PE) and E_T(30) in Scheme 4 was made by combining the E_F-versus-E_T(30) plots for **1**-O^- in polar solvents with those for **1**-O^-/H-TBA$^+$ in less polar solvents. In a polar environment whose polarity is similar to that of a polar solvent with E_T(30) in the range 45−63, $^1(OL^-)$* and a countercation make an ion pair that resembles an SSIP or a free ion couple. The emission from $^1(OL^-)$* is modulated only by the polarity of the environment, while the emission maximum varies in the small range from 625 to 640 nm. In contrast, under a less polar environment whose polarity is similar to that of a less polar solvent with E_T(30) in the range 33−45, $^1(OL^-)$* and a countercation make a CIP-like ion pair. The emission from $^1(OL^-)$* in the CIP-like ion pair is modulated by the strength of covalent character of the O8′•••H bond between $^1(OL^-)$* and the countercation as well as the polarity of the environment. Because the plot in the less polar region shows a steeper line than that in the polar region, the strength of the covalent character of the O8′•••H bond is the main factor in determining the emission maximum of OL^-. The extrapolation of the PE-versus-E_T(30) plot in the polar region into the less polar region suggests that the emission maximum of OL^- varies in the small range from 620 to 625 nm depending on the polarity of the environment, supposing that $^1(OL^-)$* is present in an ion pair resembling an SSIP or a free ion couple. Conversely, the emission maximum of OL^- in a CIP-like ion pair is modulated in the range from 541 to 620 nm by the strength of covalent character of the O8′•••H bond between $^1(OL^-)$* and the countercation. The properties of the O8′•••H bond will vary depending on the chemical properties of the countercation, such as acidity. In particular, a strong acidity of the countercation is preferable for expanding the emission wavelength range. In addition, the polarity of the environment surrounding $^1(OL^-)$* also influences the properties of the O8′•••H bond. Thus, we cannot separate these two factors, the polarity of the active-site environment and the strength of the covalent character of the O8′•••H bond between $^1(OL^-)$* and the countercation, in a CIP-like ion pair.

We apply here the light-color modulation mechanism described above to understand the origin of in vivo bioluminescence colors. The in vivo bioluminescence color varies depending on the species of firefly, click beetle, or railroad worm. The difference in the emission maxima (λ_{max} 530−640 nm) corresponds to the different properties of the active sites originating from the different amino acid sequences of the firefly (beetle) luciferases.[7−9] Among the species of fireflies and their analogous beetles, the North American firefly *Photinus pyralis* and the Japanese firefly (Genji-botaru) *Luciola cruciata* have been well-studied chemically. *P. pyralis* and *L. cruciata* generate yellow-green light. Variations in bioluminescence from green to yellow colors are typical for fireflies (beetles).[7,55] As an example of red bioluminescence, *Phrixothrix* railroad worms emit red light through head lanterns along with yellow-green light through lateral lanterns.[56] The maximum wavelengths of the in vivo bioluminescence were reported to be 562 nm for *P. pyralis*,[7,55] 544 nm for *L. cruciata*,[57] and 636 nm for the head lanterns of *Phrixothrix hirtus*.[56] According to the mechanism proposed in Scheme 4, yellow-green colors cannot be reproduced in polar media. Therefore, a less polar character must be achieved in the active sites of *P. pyralis* and *L. cruciata* luciferases to provide light emission from $^1(OL^-)$* with the respective maxima at 562 and 544 nm. Under the less polar environments of the active sites, $^1(OL^-)$* and the protonated form of a basic moiety make a CIP-like ion pair. Because the emission-maximum wavelength of *L. cruciata* (544 nm) is shorter than that of *P. pyralis* (562 nm), the active-site environment of *L. cruciata* luciferase must be less polar than that of *P. pyralis* luciferase,

(55) Seliger, H. H.; Buck, J. B.; Fasyie, W. G.; McElroy, W. D. *J. Gen. Physiol.* **1964**, *48*, 95–104.
(56) (a) Viviani, V. R.; Bechara, E. J. H. *Photochem. Photobiol.* **1993**, *58*, 615–622. (b) Viviani, V. R.; Bechara, E. J. H. *Ann. Entomol. Soc. Am.* **1997**, *90*, 389–398. (c) Viviani, V. R.; Bechara, E. J. H.; Ohmiya, Y. *Biochemistry* **1999**, *38*, 8271–8279.
(57) Kishi, Y.; Matsuura, S.; Inoue, S.; Shimomura, O.; Goto, T. *Tetrahedron Lett.* **1968**, *9*, 2847–2850.

and the strength of the covalent character of the O8′···H bond between $^1(OL^-)^*$ and the protonated basic moiety for *L. cruciata* bioluminescence must be stronger than that for *P. pyralis* bioluminescence. Specifically, *L. cruciata* luciferase must provide a nonpolar microenvironment similar to *p*-xylene or benzene solution to increase the covalent character of the O8′···H bond. In contrast, the emission maximum of *P. hirtus* (636 nm) can be reproduced in polar media according to Scheme 4. Thus, the active site of *P. hirtus* luciferase creates a polar environment, as predicted by previous work.[58] In the polar active site, $^1(OL^-)^*$ and the protonated basic moiety of *P. hirtus* luciferase form an ion pair resembling an SSIP or a free ion couple.

To rationalize the proposed light-color modulation mechanism, the existence of a basic moiety in the active sites of firefly (beetle) luciferases should be confirmed. Generally, it is known that a basic moiety is present in the active site as follows. Structural models of the active site for a ligand-bound luciferase were constructed on the basis of the crystal structure of *P. pyralis* luciferase,[15] where it is suggested that the guanidinyl side chain of Arg218 locates close to the O8′ atom of OLH.[22,59] The crystal structure of *L. cruciata* luciferase in a complex with OLH and AMP also shows that the guanidinyl side chain of Arg220 is present in the vicinity of the O8′ atom of OLH,[16] but the distances between the nitrogen atoms of the guanidinyl side chain and the O8′ atom (6.50 and 6.82 Å) may be too long for a bonding interaction. Because a guanidinyl side chain of an arginine residue has a strong basicity,[60] Arg218 of *P. pyralis* luciferase and Arg220 of *L. cruciata* luciferase play a role in protonated forms before they interact with OLH. Thus, an arginine residue at the active site may not behave as a proton acceptor for OLH, while the arginine residue plays an important role for constructing the active-site environment cooperatively. This explanation is also supported by mutation experiments on luciferases, which showed that an arginine substitution does not cause a dramatic emission-color change.[61,62] As the other basic moiety, it has been shown on the basis of crystal structure analysis of *L. cruciata* luciferase binding OLH and AMP that several amide carbonyls exist close to OLH.[16] In the crystal, the distances between the O8′ atom of OLH and the oxygen atoms of the amide carbonyls of Ser316 and Gln340 were determined to be 3.92 and 4.41 Å, respectively.[16] OLH itself is acidic enough to generate OL^- in the absence of strong bases, because generation of **1**-O^- is observed in 2-propanol, DMSO, and water in the absence of bases. Furthermore, the acidity of ^{1}OLH* is stronger than that of ground-state OLH.[32,42] Therefore, an amide moiety may have a basicity strong enough to play the role of a proton acceptor for ^{1}OLH*. While the basicity of a single amide moiety is not strong enough,[63] it is known that

Scheme 5

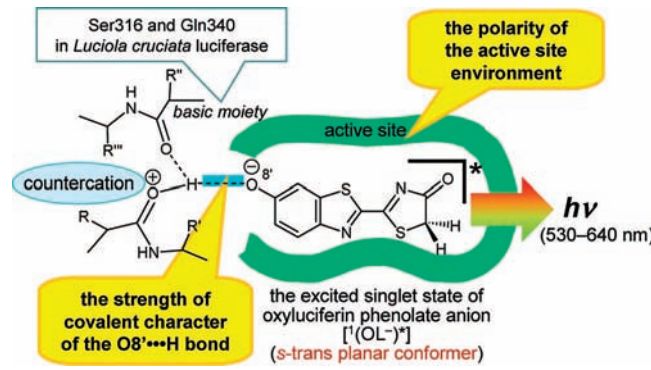

multiple amide moieties cooperate to increase the basicity.[64−66] Thus, in the case of ^{1}OLH*, multiple amide carbonyls would form a basic moiety at the active site, which successfully produces an ion pair with $^1(OL^-)^*$. In the case of *L. cruciata* luciferase, a basic moiety is formed by the amide carbonyls of Ser316 and Gln340.[16] The covalent character of the O8′···H bonds between $^1(OL^-)^*$ and protonated amide carbonyls effectively modulates the color of light emission from $^1(OL^-)^*$, as shown in Scheme 5. Protonated amide carbonyls have an acidity strong enough to obtain a wide range of bioluminescence colors.

The emission color of a luciferin−luciferase reaction in vitro is affected by environmental factors, such as pH, temperature, and the presence of additives (e.g., metal ions).[7−9,67] These environmental factors also influence the properties of an active site. To investigate the molecular function of the active site, use of mutation is a powerful methodology. A substitution of an amino acid residue in a luciferase occasionally causes a change in the bioluminescence color.[68,69] Several mechanisms have been proposed to explain the color modulation induced by a mutation. One of them is mechanism (i), which considers changes in the polarity of the active-site environment[58,70,71] and originates from the studies by Seliger and co-workers[23] and DeLuca.[24] On the basis of the present study, their mechanism should be revised. We emphasize that the bioluminescence colors are modulated not only by the polarity of the active-site environment but also by the strength of the covalent character of the O8′···H bonds between $^1(OL^-)^*$ and protonated amide carbonyls. We also reconsider mechanism (ii), which is based on the proposed resonance structures of OL^-.[22] This mechanism considers the variation of the π-electron character of OL^- in a manner similar to the mechanism proposed in the present study, but it does not consider a specific interaction between $^1(OL^-)^*$ and a countercation. Thus, mechanism (ii) should be revised by introducing a consideration of the bonding character of the interactions between $^1(OL^-)^*$ and protonated amide carbonyls. The other proposal to be reconsidered is mechanism (iii) that considers the rigidity of the active site, which regulates the

(58) Viviani, V. R.; Arnoldi, F. G. C.; Venkatesh, B.; Silva Neto, A. J.; Ogawa, F. G. T.; Oehlmeyer, T. L.; Ohmiya, Y. *J. Biochem.* **2006**, *140*, 467–474.
(59) Branchini, B. R.; Magyar, R. A.; Murtiashaw, M. H.; Anderson, S. M.; Zimmer, M. *Biochemistry* **1998**, *37*, 15311–15319.
(60) Berg, J. M.; Tymoczko, J. L., Stryer. L. *Biochemistry*, 6th ed.; Freeman: New York, 2006.
(61) (a) Viviani, V. R.; Ohmiya, Y. *Photochem. Photobiol.* **2000**, *72*, 267–271. (b) Viviani, V. R.; Uchida, A.; Viviani, W.; Ohmiya, Y. *Photochem. Photobiol.* **2002**, *76*, 538–544. (c) Viviani, V. R.; Arnoldi, F. G. C.; Ogawa, F. T.; Brochetto-Braga, M. *Luminescence* **2007**, *22*, 362–369.
(62) Branchini, B. R.; Magyar, R. A.; Murtiashaw, M. H.; Portier, N. C. *Biochemistry* **2001**, *40*, 2410–2418.
(63) Homer, R. B.; Johnson, C. D. *The Chemistry of Amides*; Zabicky, J., Ed.; Wiley-Interscience: London, 1970; pp 187−243.
(64) Wu, Z.; Fenselau, C. *J. Am. Soc. Mass Spectrom.* **1992**, *3*, 863–866.
(65) Wu, J.; Lebrilla, C. B. *J. Am. Chem. Soc.* **1993**, *115*, 3270–3275.
(66) Zhang, K.; Zimmerman, D. M.; Chung-Phillips, A.; Cassady, C. J. *J. Am. Chem. Soc.* **1993**, *115*, 10812–10822.
(67) Viviani, V. R.; Arnoldi, F. G. C.; Neto, A. J. S.; Oehlmeyer, T. L.; Bechara, E. J. H.; Ohmiya, Y. *Photochem. Photobiol. Sci.* **2008**, *7*, 159–169.
(68) Kajiyama, N.; Nakano, E. *Protein Eng.* **1991**, *4*, 691–693.
(69) Mamaev, S. V.; Laikhter, A. L.; Arslan, T.; Hecht, S. M. *J. Am. Chem. Soc.* **1996**, *118*, 7243–7244.
(70) Ugarova, N. N.; Brovko, L. Y. *Luminescence* **2002**, *17*, 321–330.
(71) Viviani, V. R.; Ohmiya, Y. *Luminescence* **2006**, *21*, 262–267.

vibrational energy loss of $^1(OL^-)^*$.[16] This hypothesis is based on a comparison of the crystal structures of the ligand-bound complexes of wild-type *L. cruciata* luciferase and its mutant. However, the proposed hypothesis should be ruled out by evidence that $^1(\mathbf{1}\text{-}O^-)^*$ has nanosecond lifetimes τ_F at room temperature. Generally, aromatic molecules in the excited singlet state deactivate via fast vibrational relaxation processes on the picosecond time scale.[72] Their finding from the crystal structure analyses is that the mutation causes a change in the distance between an LH_2 model compound and a hydrophobic side chain of an amino acid residue in the active site.[16] This structural change of the active site cannot regulate the vibrational relaxation process of $^1(OL^-)^*$. On the contrary, it causes changes in the polarity and/or the distances between $^1(OL^-)^*$ and protonated amide carbonyls during a bioluminescence reaction, resulting in a change in the strength of the covalent character of the O8′···H bonds between $^1(OL^-)^*$ and the protonated amide carbonyls.

Additionally, the molecular structure of $^1(OL^-)^*$ should be mentioned. Recent theoretical studies led to the prediction of the favored structure of $^1(OL^-)^*$ in which the benzothiazole and thiazolone rings are coplanar to one another rather than perpendicular as a result of rotation around the C2−C2′ bond.[49,54,73,74] This prediction is applicable to the cases of **1**-O^- and **1**-O^-M^+ because the π^* orbitals (LUMO or LUMO+1) of **1**-O^- and **1**-O^-M^+ for the allowed transitions have π-bonding character between C2 and C2′. Especially, the s-trans planar conformer of $^1(OL^-)^*$ is predicted to be the most stable structure in the possible conformers. The ground-state structures of OLH and **1**-OH are the s-trans planar conformers, as supported by the crystal structures of OLH bound in *L. cruciata* luciferase[16] and **1**-OH. Similarly, $^1(\mathbf{1}\text{-}O^-)^*$ exists as the s-trans planar conformer, which corresponds to the major component observed in the fluorescence lifetime measurements. While our study cannot determine the molecular structure of $^1(\mathbf{1}\text{-}O^-)^*$ directly, the s-trans planar conformer is plausible for $^1(OL^-)^*$ during the bioluminescence.

Conclusions

We have systematically investigated the spectroscopic properties of phenolate anion **1**-O^- in various solvents containing an organic base in order to reveal the light-color modulation mechanism of the firefly (beetle) bioluminescence. Phenolate anion **1**-O^- was used as a model compound of the keto form of wild-type oxyluciferin phenolate anion (OL^-), which is postulated to be the most plausible candidate for the structure of the light emitter of the bioluminescence.[21] The spectroscopic properties of the neutral form **1**-OH and the methyl ether derivative **1**-OCH_3 were also investigated for comparison. From the results, it was found that the fluorescence emission maximum (λ_F) of **1**-O^- varied in the range from 541 to 640 nm depending on the solvent polarity and the bonding interaction between $^1(\mathbf{1}\text{-}O^-)^*$ and a countercation (the conjugate acid of the organic base). In a polar solvent, $^1(\mathbf{1}\text{-}O^-)^*$ and the countercation form an SSIP or a free ion couple, and the polarity of the solvent modulates the λ_F values of **1**-O^- in the range from 625 to 640 nm. In a less polar solvent, a CIP of $^1(\mathbf{1}\text{-}O^-)^*$ and the countercation is formed. In the CIP, the solvent polarity and the strength of the covalent character of the O8′···H bond between $^1(\mathbf{1}\text{-}O^-)^*$ and the countercation modulate the λ_F value of **1**-O^- in the range from 540 to 625 nm. The fluorescence lifetime analyses of **1**-O^- also revealed that the emission properties of $^1(\mathbf{1}\text{-}O^-)^*$ depend on the solvent polarity and the ion-pair structures. DFT calculations on **1**-O^- and the ion-pair models **1**-O^-M^+ support the idea that the λ_F value of **1**-O^- can be modulated as a function of the strength of the covalent character of the O8′···H bond between $^1(\mathbf{1}\text{-}O^-)^*$ and the countercation. Because the calculated results showed that the two methyl groups at C5 of **1**-O^- have little effect on the π-electron properties of **1**-O^-, we extrapolated the spectroscopic properties of **1**-O^- determined here to those of OL^-. On the basis of the result that the range of the λ_F value of **1**-O^- covers almost the whole range of the bioluminescence emission (530 to 640 nm),[7−9] it is possible to conclude that the light-emitting center of the firefly (beetle) bioluminescence is the excited singlet state of the keto form of oxyluciferin phenolate anion, $^1(OL^-)^*$. Thus, we propose the following light-color modulation mechanism for the firefly (beetle) bioluminescence: (1) the light emitter is $^1(OL^-)^*$, and (2) the wavelength of the light emission from $^1(OL^-)^*$ is modulated by the polarity of the active-site environment of a luciferase and the degree of covalent character of the O8′···H bond between $^1(OL^-)^*$ and a protonated basic moiety in the active site.

On the basis of the spectroscopic properties of **1**-O^-, we depict a road map for understanding the bioluminescence color variation as a function of a solvent-polarity parameter, $E_T(30)$, as shown in Scheme 4. Consideration of the proposed road map for understanding the mechanism of the in vivo bioluminescence colors of *P. pyralis*, *L. cruciata*, and *P. hirtus* leads to predictions of the polarities of the active-site environments of their luciferases and the bonding characters of the interactions between $^1(OL^-)^*$ and protonated basic moieties. It is predicted that stronger acidity of the protonated basic moiety in a luciferase leads to expansion of the color-variation range. The potential basic moiety may consist of multiple amide carbonyls in the active site. In the case of *L. cruciata* luciferase, the active site has a nonpolar character similar to *p*-xylene and benzene solutions, and the amide carbonyls of Ser316 and Gln340 play an important role as basic moieties (Scheme 5). Additionally, the structure of $^1(OL^-)^*$ for the firefly (beetle) bioluminescence is postulated to be the s-trans planar conformer.

Experimental Section

Instruments and Computations. Melting points were obtained with a Yamato MP-21 apparatus. IR spectra were measured with a Horiba FT-720 spectrometer. Electron ionization mass spectrometry (EI-MS) and high-resolution electrospray ionization mass spectrometry (HR-ESI-MS) were performed using JEOL JMS-600 and JEOL JMS-T100LC mass spectrometers, respectively. ^1H NMR spectra were recorded on a JEOL GX-270 instrument (270 MHz). UV−vis absorption spectra were recorded on a Varian Cary 50 spectrophotometer (scan speed, 600 nm/min; data interval, 1 nm). Fluorescence spectra were measured with a JASCO FP-6500 fluorescence spectrophotometer. It was confirmed that the excitation spectrum of the fluorescence agreed with the corresponding absorption spectrum. Fluorescence quantum yields were determined by comparing the corrected fluorescence spectra with that of quinine sulfate in 0.10 M H_2SO_4 ($\Phi_F = 0.546$, $\lambda_{ex} = 366$ nm) as the standard.[75] Spectroscopic measurements were made in a quartz cuvette (1 cm path length) at 25 ± 1 °C. Spectral-grade solvents were used for measure-

(72) Turro, N. J. *Modern Molecular Photochemistry*; University Science Books: Sausalito, CA, 1991.
(73) Nakatani, N.; Hasegawa, J.; Nakatsuji, H. *J. Am. Chem. Soc.* **2007**, *129*, 8756–8765.
(74) Liu, Y.-J.; De Vico, L.; Lindh, R. *J. Photochem. Photobiol., A* **2008**, *194*, 261–267.

Scheme 6. Synthesis of **1**-OH and **1**-OCH_3

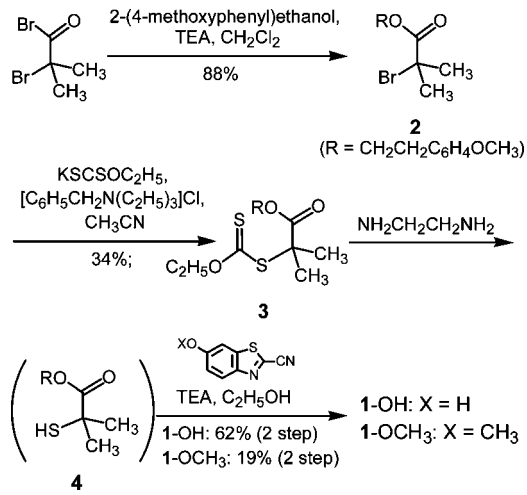

ments of UV−vis absorption and fluorescence. Nanosecond fluorescence lifetimes were determined by using a time-correlated single-photon-counting fluorimeter (Edinburgh Analytical Instruments, FL-900CDT). The fluorescence time profiles were analyzed by deconvolution with the instrumental response function. The details of the photon-counting systems are described elsewhere.[76] Appropriate cutoff filters were used in order to avoid second generation of excitation and emission light. Quantum-chemical calculations were performed using the Gaussian 03 program[50] on the computer system of the Information Technology Center of UEC. We used DFT with Becke's three-parameter functional[51] combined with Lee, Yang, and Parr's correlation functional[52] (B3LYP) along with a 6-31+G(d) basis set.[53] Molecular graphics were generated using GaussView, version 3.09.[77]

Synthesis of 5,5-Dimethyloxyluciferin (1-OH) and Its Methyl Ether Derivative (1-OCH_3). Compounds **1**-OH and **1**-OCH_3 were prepared by the procedure shown in Scheme 6.

Synthesis of 2-(4-Methoxyphenyl)ethyl 2-Bromoisobutyrate (2). To a solution of 2-(4-methoxyphenyl)ethanol (0.99 mL, 8.0 mmol) and 2-bromoisobutyryl bromide (1.21 g, 8.0 mmol) in dichloromethane (10 mL), triethylamine (1.3 mL, 9.3 mmol) was added at 0 °C under Ar. After the mixture was stirred at 0 °C for 1 h, the reaction was quenched by the addition of water, and the product was extracted with ethyl acetate. The organic layer was washed with brine, dried over Na_2SO_4, and concentrated in vacuo to give **2** (2.11 g, 88%) as colorless oil. IR (neat): 3003, 2956, 2933, 2835, 1736, 1514, 1248, 1161 cm^{-1}. ^1H NMR ($CDCl_3$, 270 MHz): δ 1.90 (6H, s), 2.93 (2H, t, J = 6.9 Hz), 3.80 (3H, s), 4.34 (2H, t, J = 6.9 Hz), 6.85 (2H, AA′BB′), 7.16 (2H, AA′BB′). EI-MS m/z (%): 302 (M^+, 1.3), 300 (M^+, 1.2), 134 (100), 121 (24).

Synthesis of *O*-Ethyl *S*-2-[2-(4-Methoxyphenyl)ethoxycarbonyl]-2-propyldithiocarbonate (3). Bromoisobutyrate **2** (2.01 g, 6.70 mmol), potassium *O*-ethyl dithiocarbonate (1.37 g, 8.56 mmol), and benzyltriethylammonium chloride (1.83 g, 8.02 mmol) were dissolved in acetonitrile (15 mL) under Ar, and the mixture was stirred at room temperature for 5 h. The reaction was quenched by the addition of water, and the product was extracted with ethyl acetate. The organic layer was washed with brine, dried over Na_2SO_4, and concentrated in vacuo. The residue was purified by column chromatography (SiO_2, hexane/ethyl acetate) to give **3** (771 mg, 34%) as a yellow oil accompanied by the recovered ester (908 mg, 40%). IR (neat): 2979, 2954, 2935, 2835, 1734, 1514, 1246, 1157, 1047 cm^{-1}. ^1H NMR ($CDCl_3$, 270 MHz): δ 1.29 (3H, t, J = 7.3 Hz), 1.57 (6H, s), 2.89 (2H, t, J = 6.9 Hz), 3.79 (3H, s), 4.28 (2H, t, J = 6.9 Hz), 4.47 (2H, q, J = 7.3 Hz), 6.83 (2H, AA′BB′), 7.14 (2H, AA′BB′). EI-MS m/z (%): 342 (M^+, 3.4), 278 (4.5), 134 (100), 121 (11).

Synthesis of 1-OH. Dithiocarbonate **3** (194 mg, 0.57 mmol) was dissolved in ethylenediamine (2.8 mL) under Ar, and the reaction mixture was stirred at room temperature for 110 min. The reaction was quenched by the addition of saturated aqueous NH_4Cl solution, and 2-(4-methoxyphenyl)ethyl 2-mercaptoisobutyrate (**4**) was extracted with ether. The organic layer was washed with brine, dried over Na_2SO_4, and concentrated in vacuo. The residue containing **4** (144 mg) was dissolved in ethanol (3 mL) under Ar, and 2-cyano-6-hydroxybenzothiazol (58 mg, 0.33 mmol) and triethylamine (90 μL, 0.65 mmol) were added to the solution. The mixture was heated at reflux for 6.5 h and then cooled to room temperature. The reaction mixture was purified by TLC (SiO_2, $CHCl_3$/hexane/methanol) to give **1**-OH (54 mg, 35%) as a yellow powder. Mp: 279−281 °C (lit.[18] 280−283 °C). IR (KBr): 3190, 2929, 1723, 1603, 1493, 1466, 1228 cm^{-1}. ^1H NMR (CD_3OD, 270 MHz): δ 1.70 (6H, s), 7.14 (1H, dd, J = 2.3, 9.2 Hz), 7.40 (1H, d, J = 2.3 Hz), 8.02 (1H, d, J = 9.2 Hz). EI-MS m/z (%): 278 (M^+, 100), 263 (25), 194 (40). HR-ESI-MS (m/z): calcd for $C_{12}H_{11}N_2O_2S_2$ [M + H]$^+$, 279.0262; found, 279.0262.

Synthesis of 1-OCH_3. Dithiocarbonate **3** (391 mg, 1.08 mmol) was dissolved in ethylenediamine (6 mL) under Ar, and the reaction mixture was stirred at room temperature for 3.5 h. The reaction was quenched by the addition of saturated aqueous NH_4Cl solution, and **4** was extracted with ether. The organic layer was washed with brine, dried over Na_2SO_4, and concentrated in vacuo. To the residue containing **4**, 2-cyano-6-methoxybenzothiazol (190 mg, 1.00 mmol) and triethylamine (250 μL, 1.8 mmol) were added, and the mixture was dissolved in ethanol (7 mL) under Ar. The mixture was heated at reflux for 20 h and then cooled to room temperature and concentrated in vacuo. The residue was purified by column chromatography (SiO_2, hexane/ethyl acetate) and TLC (SiO_2, first with toluene/ethyl acetate and then with $CHCl_3$/hexane/ethyl acetate) to give **1**-OCH_3 (55 mg, 19%) as yellow needles. Mp: 185 °C (sublimation). IR (KBr): 2979, 2939, 1728, 1606, 1533, 1479, 1227 cm^{-1}. ^1H NMR (CD_3OD, 270 MHz): δ 1.71 (6H, s), 3.94 (3H, s), 7.26 (1H, dd, J = 2.3, 8.9 Hz), 7.67 (1H, d, J = 2.3 Hz), 8.08 (1H, d, J = 8.9 Hz). EI-MS m/z (%): 292 (M^+, 100), 278 (41), 259 (23), 208 (45). HR-ESI-MS (m/z): calcd for $C_{13}H_{13}N_2O_2S_2$ [M + H]$^+$, 293.0418; found, 293.0427.

Acknowledgment. This work was supported by a grant from the Ministry of Education, Culture, Sports, Science, and Technology of Japan. We acknowledge technical assistance with the quantum-chemical calculations from the Information Technology Center of UEC.

Supporting Information Available: ^1H NMR spectra of all of the compounds; single-crystal X-ray data for **1**-OH and **1**-OCH_3 in CIF format; Gaussian-fit analyses of the fluorescence spectra of **1**-O^-; fluorescence decays obtained by time-correlated single-photon counting measurements; optimized structures calculated by DFT; and complete ref 50. This material is available free of charge via the Internet at http://pubs.acs.org.

JA808836B

(75) Eaton, D. F. *Pure. Appl. Chem.* **1988**, *7*, 1107–1114.
(76) Yamaji, M. *Photochem. Photobiol. Sci.* **2008**, *7*, 711–717.
(77) Dennington, R., II; Keith, T.; Millam, J.; Eppinnett, K.; Hovell, W. L.; Gilliland, R. *GaussView*, version 3.09; Semichem, Inc.: Shawnee Mission, KS, 2003.